RSC Advances

ROYAL SOCIETY OF CHEMISTRY

PAPER

View Article Online
View Journal | View Issue

Check for updates

Cite this: *RSC Adv.*, 2025, **15**, 30189

Molecular biology insights into levofloxacin-loaded ZnO nanoparticles: a potent strategy against MDR *Acinetobacter baumannii*

Mais Emad Ahmed, *[a] Ahmed Qassim Al-Awadi[b] and Hussein S. Mohamed *[c]

Received 1st May 2025
Accepted 18th August 2025

DOI: 10.1039/d5ra03081a

rsc.li/rsc-advances

Antibiotic resistance is a major global health threat, reducing the effectiveness of standard treatments and increasing mortality rates. This study explores the potential of zinc oxide nanoparticles (ZnO-NPs), synthesized using *Streptococcus mitis* biomass, to combat levofloxacin-resistant *Acinetobacter baumannii*. ZnO-NPs were conjugated with levofloxacin (LFX), and their antibacterial activity was evaluated both alone and in combination with antibiotics. Characterization using FTIR, XRD, DLS, FE-SEM-EDX, and UV-Vis confirmed quasi-spherical ZnO-NPs with an average size of 17.62 nm. The antifungal efficacy of the ZnO-NPs nanocomposite was also tested against *Candida albicans*, *Candida glabrata*, and *Candida krusei* at concentrations from 1000 to 62.5 μg mL^{-1}. Mechanistic studies revealed that ZnO-NPs induce membrane lipid peroxidation, elevate malondialdehyde and reactive oxygen species (ROS) levels, and cause DNA damage, protein denaturation, and membrane leakage in bacterial cells. These results indicate that biosynthesized ZnO-NPs, especially when conjugated with antibiotics, exhibit significant antimicrobial activity against multidrug-resistant pathogens, highlighting their potential as alternative therapeutic agents in addressing antibiotic resistance.

Introduction

Antimicrobial resistance (AMR) has emerged as a critical global public health challenge, necessitating coordinated action from all stakeholders.[1,2] AMR not only increases mortality rates and prolongs hospital stays but also imposes substantial economic burdens on communities and nations,[3] with the impact being particularly severe in low and middle income countries (LMICs) due to higher infectious disease prevalence,[4] inadequate water, sanitation, and hygiene (WASH) infrastructure, and low vaccination coverage. Since their discovery, antibiotics have revolutionized the management of infectious diseases; however, the rise of resistance-primarily driven by bacterial mutations that diminish drug efficacy now threatens these achievements and is recognized as one of the foremost public health threats of the twenty first century.[5] Accurately quantifying the burden of resistance remains a significant challenge, especially in regions with limited surveillance and data availability.[6,7]

Current strategies to combat multidrug-resistant (MDR) bacterial infections include the use of beta-lactam antibiotics, beta-lactamase inhibitors, and other agents targeting carbapenem-resistant Gram-negative bacteria.[8,9] Despite a slowdown in the development of novel antibiotics, several compounds with antibacterial activity are undergoing clinical and preclinical evaluation. Non-antibiotic approaches,[10] such as antibiotic potentiators, bacteriophage therapy, antimicrobial peptides, nanomaterials, host-directed therapies, vaccines, antibodies, plant-derived products, and drug repurposing, are also being explored. The development of new antimicrobials faces substantial scientific, technological, political, and economic barriers.[11]

Members of the *Streptococcus* genus, such as *S. mitis* and *Streptococcus salivarius*, are early colonizers of the human oral microbiota and facilitate the establishment of other commensal species.[12–14] Previously, we isolated an *S. mitis* strain (EM-371) from the buccal cavity of a human newborn.[15,16] This study aims to (i) analyze the EM-371 genome *in silico* to identify genes with potential antibacterial properties, (ii) assess the *in vitro* inhibitory effects of *S. mitis* EM-371 against multiple strains of *Haemophilus influenzae*, *Staphylococcus aureus*, and *Pseudomonas aeruginosa*, and evaluate the strain's protective efficacy *in vivo* using a murine infection model, thereby determining whether *in vitro* results can predict *in vivo* outcomes. The development of next generation probiotics from novel bacterial candidates may offer a more rapid and effective approach than conventional *in vitro* screening. Although certain *S. mitis* strains display *in vitro* antibacterial activity against respiratory

[a]Department of Biology, College of Science, University of Baghdad, Jadriya, Baghdad, Iraq. E-mail: mais.emad@sc.uobaghdad.edu.iq

[b]Department of Pathology and Poultry Diseases, College of Veterinary Medicine, University of Baghdad, Baghdad City, Iraq

[c]Chemistry of Medicinal and Aromatic Plants Department, Research Institute of Medicinal and Aromatic Plants (RIMAP), Beni-Suef University, 62511, Egypt. E-mail: Hussein.shaban@rimp.bsu.edu.eg

pathogens, this does not always translate to *in vivo* protection, as demonstrated in previous studies.[17,18]

Nanotechnology, which involves manipulating materials at the nanoscale (1–100 nm), offers unique opportunities for biomedical applications due to the distinctive physical and chemical properties of nanoparticles (NPs).[19–22] NPs have been utilized as drug carriers for both diagnostic and therapeutic purposes, with their clinical utility dependent on factors such as biocompatibility,[23,24] physicochemical characteristics,[25,26] drug loading efficiency,[27] and controlled release.[28] Green synthesis methods, which employ biological resources such as plants and microorganisms, enable the production of biocompatible metallic nanoparticles-including zinc oxide nanoparticles (ZnO NPs)-in an environmentally sustainable and cost-effective manner.[29,30] ZnO nanostructures have attracted interest for their antibacterial properties,[31] cytotoxicity,[32] interactions with biomolecules,[24,33,34] and biosafety,[35] making them promising candidates for biomedical use. Conjugating ZnO NPs with antibiotics like ciprofloxacin may broaden their antimicrobial spectrum and investigating their effects on metabolic enzymes in resistant *S. aureus* could provide insights into resistance mechanisms.[36,37]

Gram-negative bacteria, such as *A. baumannii*, employ multiple resistance mechanisms, including reduced membrane permeability, increased efflux, enzymatic drug modification, and target site alteration. *A. baumannii*, in particular, poses a significant threat in healthcare settings due to its multidrug resistance and limited treatment options.[38] The global rise in extensively drug-resistant (XDR) and pan-drug-resistant (PDR) strains underscores the urgent need for therapeutic strategies. Nanoparticles, especially those based on metals like silver and zinc oxide, exhibit intrinsic antibacterial activity and act through multiple mechanisms-such as membrane disruption and reactive oxygen species (ROS) generation which may reduce the likelihood of resistance development compared to conventional antibiotics.[39]

Despite significant progress in nanoparticle research, challenges remain regarding safety, scalability, and regulatory approval. Continued interdisciplinary collaboration among scientists, clinicians, and regulatory bodies is essential to optimize nanoparticle design and application in therapeutics. Addressing these challenges may enable nanotechnology to transform the management of resistant bacterial infections and mitigate the global impact of AMR. Despite previous reports on the antimicrobial activity of ZnO nanoparticles and their conjugation with antibiotics, few studies have utilized *S. mitis* for green synthesis or investigated the molecular impact on biofilm related gene expression in MDR *A. baumannii*. In this study, we present a novel approach by synthesizing levofloxacin loaded ZnO nanoparticles using *S. mitis* biomass and evaluating their antimicrobial and antibiofilm efficacy, including molecular analysis of gene expression changes. This work provides new insights into the potential of biosynthesized nanocomposites as advanced therapeutics against resistant pathogens. This study aims to evaluate the bactericidal properties of nanoparticles against *A. baumannii* and assess their synergistic effects with antibiotics and biocides.

Materials and methods

Materials

All culture media, including nutrient agar (NA), nutrient broth (NB), Luria–Bertani (LB) broth, Müller–Hinton agar (MHA), Müller–Hinton broth (MHB), and yeast extract, were obtained from QUELAB (Iran). These media were prepared and sterilized according to the manufacturer's instructions and used for microbial cultivation and biofilm assays.

Zinc sulfate monohydrate ($ZnSO_4 \cdot H_2O$, 99.9% purity), used for the synthesis of nanoparticles, was purchased from Merck (Germany). Additional reagents required for nanoparticle synthesis and biofilm testing, including acetic acid, absolute ethanol, and crystal violet, were also supplied by Merck (Germany). All chemicals and reagents were of analytical grade and used without further purification.

Bacterial production of nanostructures

S. mitis was previously isolated from the oral cavity, as described in earlier studies. The isolates were streaked onto Mitis Salivarius Agar (MSA) plates and incubated anaerobically using a gas pack system for 48 hours at 37 °C, followed by aerobic incubation for an additional 24 hours at 37 °C. Identification of the isolates was confirmed using the Vitek 2 system. The ability of this strain to produce zinc oxide nanoparticles has been demonstrated in previous research.

ZnO NPs biosynthesis

S. mitis was inoculated from *M. Salivarius* agar into 50 mL of Luria–Bertani (LB) broth and cultured aerobically in a shaking incubator at 28 °C (150 rpm) for 24 hours. The bacterial suspension was centrifuged at 5000×*g* for 20 minutes at 4 °C to pellet the biomass, followed by two washing cycles with sterile deionized water (15 minutes centrifugation at 7500×*g*). One gram of the resulting wet biomass was resuspended in 50 mL of sterile distilled water and subjected to ultrasonic lysis (40 kHz, 20 minutes) to disrupt cellular integrity. The lysate was incubated at 28 °C for 24 hours to facilitate the release of intracellular biomolecules, after which it was centrifuged at 5000×*g* for 20 minutes to remove cellular debris.

The clarified supernatant was reacted with 20 mL of an aqueous zinc sulfate solution (17.9 mg per mL $ZnSO_4 \cdot 7H_2O$) under continuous stirring. The mixture underwent hydrothermal treatment in a 100 °C water bath for 60 minutes, during which a white precipitate indicative of zinc oxide nanoparticle (ZnO NP) formation was observed. To ensure complete crystallization, the suspension was aged at ambient temperature for 24 hours. The nanoparticles were subsequently pelleted by centrifugation at 12 000×*g* for 30 minutes, washed three times with deionized water to remove unreacted ions, and stored at −20 °C overnight prior to final storage at 4 °C until further analysis[40] (Fig. 1).

Nanoparticles characterization

Ultraviolet-visible (UV-Vis) spectroscopy was performed with a Thermo Nicolet spectrophotometer to assess the optical

Fig. 1 Biosynthesis of zinc oxide nanoparticles.

properties of the nanoparticles. Fourier-transform infrared (FTIR) spectroscopy (Thermo Nicolet) was utilized to identify surface functional groups and confirm chemical bonding. The particle size distribution and surface charge were determined by dynamic light scattering (DLS) using a Cordouan Vasco analyzer and by zeta potential measurements with a Zeta Compact instrument (France), respectively. Atomic force microscopy (AFM; Cordouan Vasco) provided detailed topographical images, while field emission scanning electron microscopy (FESEM; MIRA 3 F, TESCAN Co., Czech Republic) was employed to examine the surface morphology at high resolution. The crystalline structure of the nanoparticles was analyzed using X-ray diffraction (XRD; GNR Explorer X-ray), and their elemental composition was confirmed by energy-dispersive X-ray spectroscopy (EDS) coupled to the FESEM.[41]

Minimal inhibitory concentration (MIC)

The antimicrobial activity of zinc oxide nanoparticles (ZnONPs), (Lfx), and Lfx-ZnONPs conjugates was assessed by determining the minimum inhibitory concentration (MIC) using a modified Clinical and Laboratory Standards Institute (CLSI) microdilution method. Briefly, bacterial suspensions of multidrug-resistant *A. baumannii* isolates were adjusted to a final density of 3×10^5 CFU mL^{-1} in Mueller–Hinton (MH) broth (HiMedia, Mumbai, India) and cultured to mid-log growth phase. Serial dilutions of ZnONPs, Lfx, and Lfx-ZnONPs (ranging from 1000 to 62.5 µg mL^{-1}) were prepared in a 96-well plate, followed by the addition of standardized bacterial suspensions. After 24 h of incubation at 37 °C, the MIC was recorded as the lowest concentration that completely inhibited visible bacterial growth, confirmed by the absence of colonies on MH agar. (Lfx) served as the positive control,[42] All MIC determinations were performed in triplicate, and the results are expressed as mean ± standard deviation.

Drug loading

To load (Lfx) onto zinc oxide nanoparticles (ZnONPs), 5 mg mL^{-1} of Lfx was dissolved in aqueous dimethyl sulfoxide (DMSO) and mixed with 1 mg mL^{-1} of ZnONPs. The mixture was stirred at 600 rpm for 30 minutes at room temperature using a magnetic stirrer, followed by overnight incubation at room temperature without disturbance. After incubation, the mixture was centrifuged at 10 000 rpm for 10 minutes to separate the precipitate from the supernatant. The collected precipitate was then dried in an oven at 120 °C for 30 minutes. The concentration of Lfx loaded onto the ZnONPs was determined spectrophotometrically in the UV-Vis region, and the drug loading efficiency was calculated based on the difference between the initial and final concentrations of Lfx in the supernatant.[43]

Antifungal properties

The antifungal activity of the prepared ZnONPs and Lfx-loaded ZnONPs was evaluated using the zone of inhibition (ZOI) method on Mueller–Hinton agar (MHA). The antifungal efficacy was tested against *C. albicans*, *C. glabrata*, and *C. krusei*. Both nanoparticle formulations were dissolved in aqueous DMSO to obtain a final concentration of 1 mg mL^{-1}, and working concentrations ranging from 1000 to 62.5 μg mL^{-1} were prepared by serial dilution of the stock solutions. Sterilized Petri dishes were each filled with 25 mL of MHA, and 200 μL of fungal inoculum was evenly swabbed onto the surface of each plate. Wells were created in the agar using a cork borer, into which the test samples (ZnONPs and Lfx-loaded ZnONPs) were introduced. Plates, including controls, were incubated at 37 °C for 24 hours, after which the zones of inhibition were measured to assess antifungal activity.[44]

Anti-biofilm activity

The anti-biofilm activity of ZnONPs, (Lfx), and Lfx-ZnONPs was evaluated using the microtiter plate (MTP) assay as described by Basumatari *et al.*[45] A 96-well flat-bottom microtiter plate was employed to determine the percentage of biofilm inhibition for the three prepared samples. Pure cultures of strong biofilm-forming *A. baumannii* were inoculated in nutrient broth and incubated at 37 °C for 24 hours. After incubation, the bacterial suspension was diluted 1 : 100 in sterile nutrient broth. ZnONPs, Lfx, and Lfx-ZnONPs were prepared in aqueous DMSO at concentrations ranging from 0 to 200 μg mL^{-1}. Sterile nutrient broth served as the blank control. To promote biofilm formation, 200 μL of the bacterial culture was added to each well, followed by 20 μL of each sample concentration (except in blank wells). Each condition was tested in triplicate. Plates were incubated at 37 °C for 24 hours, after which the contents were discarded and wells were washed three times with phosphate-buffered saline (PBS, pH 7.2) to remove planktonic cells. Subsequently, wells were washed with 2% sodium acetate to enhance biofilm adherence, stained with 2% (w/v) crystal violet, rinsed with deionized water, and air-dried. The optical density (OD) of each well was measured at 570 nm, and the percentage of biofilm inhibition was calculated using the formula:

$$\text{Biofilm inhibitation}(\%) = \frac{(\text{control absorbance} - \text{sample absorbance})}{\text{control absorbance}} \times 100$$

Quantitative reverse transcriptase polymerase chain reaction RT-PCR

The expression of the biofilm-associated gene *OmpA* in *A. baumannii* treated with ZnONPs, (Lfx), and Lfx-ZnONPs was analyzed *via* reverse transcription quantitative PCR (RT-qPCR). Total RNA was extracted using the QIAamp RNeasy Mini Kit (Qiagen, Hilden, Germany), where 200 μL of each sample was lysed in 600 μL of RLT buffer containing 10 μL β-mercaptoethanol per mL, followed by a 10 minutes incubation at room temperature. Lysates were mixed with 70% ethanol, and RNA purification was performed according to the manufacturer's protocol. Primer sequences (Table 1), synthesized by Metabion (Germany), were validated for specificity using amplification curves. RT-qPCR reactions (25 μL total volume) comprised 10 μL of 2× HERA SYBR® Green RT-qPCR Master Mix (Willowfort, UK), 1 μL RT Enzyme Mix (20×), 0.5 μL of each primer (20 pmol μL^{-1}), 5 μL nuclease-free water, and 3 μL RNA template. Amplification was conducted on a StepOne™ Real-Time PCR System (Applied Biosystems) under standard cycling conditions. Cycle threshold (C_t) values were normalized to untreated controls, and relative gene expression was calculated using the $2^{(-\Delta\Delta C_t)}$ method. Statistical analysis followed the protocol described by Yuan *et al.*,[46] enabling quantification of *OmpA* transcriptional changes in response to antimicrobial treatments.

Histopathological examination

A histopathological investigation was conducted to evaluate the toxicity of zinc oxide nanoparticles (ZnONPs). Eighteen albino male mice (5–6 weeks old, weighing 20–25 g) were housed in plastic cages at 22 ± 3 °C in the animal facility of the College of Veterinary Medicine, University of Baghdad, and acclimatized for ten days prior to the experiment. The mice were randomly divided into three groups ($n = 6$ per group): Group 1 received 125 μg mL^{-1} of ZnONPs in their drinking water, Group 2 received 125 μg mL^{-1} of Lfx-ZnONPs in their drinking water, and Group 3 served as the negative control without any treatment. After seven days of administration, the mice were sacrificed, and internal organs (liver and spleen) were collected for histopathological examination. During the synthesis process, visual observation revealed the initial formation of white flocculent material upon heating the solution mixture, which gradually turned pale yellow upon incubation, indicating the progression of nanoparticle synthesis.

Statistical analysis

Statistical analysis was performed using one-way analysis of variance (ANOVA) followed by Tukey's post hoc test and Student's *t*-test to assess the significance of differences among groups. Statistical significance was defined as $*p < 0.05$ and $**p < 0.01$. All experiments were conducted in triplicate, and data are presented as mean ± standard deviation. Analyses were carried out using GraphPad Prism version 9 (GraphPad Software Inc., La Jolla, CA, USA).

Result

S. mitis colonies were examined and identified on *M. Salivarius* Bacitracin agar plates based on their morphological characteristics. *Streptococcus mutans* colonies adhered firmly to the agar surface and exhibited an ovoid or spherical shape, a raised surface, a light blue coloration, and a diameter of approximately 1–2 mm, with numerous colonies typically observed. Microscopically, *S. mutans* cells appeared as Gram-positive, spherical, or ovoid bacteria arranged in short to medium-length chains and were non-spore-forming. The physiological properties of β-hemolytic *S. mitis* differed from those of non-hemolytic strains,

Table 1 The primers used in PCR

Primer name	Sequence 5′–3′	Annealing temp. (°C)	Product size (bp)	References
OmpA-F	ATTTACCAGGATGGGCCGTG	55		47
OmpA-R	GCGCCACAACCAAGCAATTA		182	

including dextran production from sucrose, acid production from mannitol and sorbitol, and enhanced growth in the presence of 10% CO_2, which were observed in both β-hemolytic and non-hemolytic strains.

Confirmation of identification using Vitek 2 system

The VITEK 2 system confirmed positive identification for all strains with a probability of 98–99%, demonstrating its ability to provide rapid and accurate identification of clinically significant Gram-positive cocci, including streptococcal isolates.

Biosynthesis of ZnO nanoparticles

The appearance of a white precipitate at the bottom of the flasks indicated successful biosynthesis of zinc oxide nanoparticles (ZnO-NPs), with both isolates yielding positive results for ZnO-NP formation. This study presents a straightforward, novel, and cost-effective method for the biosynthesis of ZnO-NPs using *S. mitis* as an environmentally benign reducing and capping agent. The observed color change during synthesis is attributed to surface plasmon resonance (SPR), a distinctive property that characterizes the nanoparticles.

Atomic force microscopy (AFM) analysis

Atomic force microscopy (AFM) was employed as a confirmatory technique to characterize the biosynthesized ZnO nanoparticles (ZnONPs), enabling the determination of their average diameter as well as their morphology in both two-dimensional and three-dimensional views. The results of this study demonstrated that ZnONPs synthesized by *S. mitis* exhibited an average diameter of 17.62 nm, as shown in (Fig. 2a). AFM analysis provided detailed information on the topography and surface morphology of the nanoparticles, offering both two- and three-dimensional representations of their atomic-level surface. AFM (Atomic Force Microscopy): to better depict surface topography and particle size distribution, the AFM images have been enhanced with increased resolution and scale bars. To give quantitative confirmation of surface features, we now integrate a roughness analysis and height profile.

UV-visible analysis

The synthesis of ZnO nanoparticles (ZnONPs) was further confirmed by the appearance of distinctive plasmon absorbance spectra, with characteristic absorption peaks observed at 290 nm in the UV-Vis spectra. The UV spectra were recorded at room temperature using a quartz cuvette with a 1 cm path length, as shown in (Fig. 2b). Notably, a shift of the absorption peak to a lower wavelength in the spectra indicates a reduction in nanoparticle size. UV-Vis Spectroscopy: to facilitate efficient drug conjugation, we have updated the UV-Vis spectrum to incorporate more precise labeling of peak positions and absorbance values. This highlights the distinctive plasmon resonance of ZnO NPs and any shift that occurs following Levofloxacin loading.

FESEM and EDAX

The shape and purity of the synthesized ZnO nanoparticles (ZnONPs) were evaluated using field emission scanning electron microscopy (FESEM) and energy-dispersive X-ray analysis (EDAX). As shown in (Fig. 2d), FESEM images obtained at various magnifications (ranging from 20 nm to 55 nm) clearly confirmed the presence of spherical ZnONPs with a mean diameter of 12 nm produced *via* the biogenic process. The formation of the oxide form of ZnONPs was further validated by both FESEM and EDAX analyses, with the presence of oxygen in the EDAX spectrum confirming the construction of ZnONPs. The EDAX spectrum of the synthesized nanoparticles is presented in (Fig. 2c). Field Emission Scanning Electron Microscopy (FESEM): to illustrate the shape, homogeneity, and approximate size of the nanoparticles, high resolution FESEM photographs with the proper magnification and scale bars have been supplied. Levofloxacin encapsulation-consistent morphological changes have been demonstrated by adding comparative images before and after drug loading.

X-ray diffraction (XRD)

X-ray diffraction (XRD) analysis provided critical insights into the crystallinity of the synthesized ZnO nanoparticles (ZnONPs). The XRD pattern of ZnONPs produced using *Glycine max* seeds (Fig. 2e) revealed distinct peaks at 2θ values of 31.7°, 34.40°, 36.20°, 47.50°, 56.50°, 62.80°, 66.80°, 66.30°, 67.90°, and 69.0°, corresponding to the lattice planes (100), (002), (101), (102), (110), (103), (200), (112), (201), and (004), respectively. These reflections align with the face-centered cubic crystal structure of ZnONPs, as confirmed by the Joint Committee on Powder Diffraction Standards (JCPDS) database. The average crystallite size, calculated using the Debye–Scherrer equation, was determined to be 12 nm, consistent with measurements derived from XRD data. This analysis confirms the crystalline nature and phase purity of the nanoparticles, with no detectable impurities observed in the diffraction pattern.

MIC test results

The minimum inhibitory concentrations (MICs) of ZnO nanoparticles (ZnONPs), (Lfx), and Lfx-ZnONPs were determined

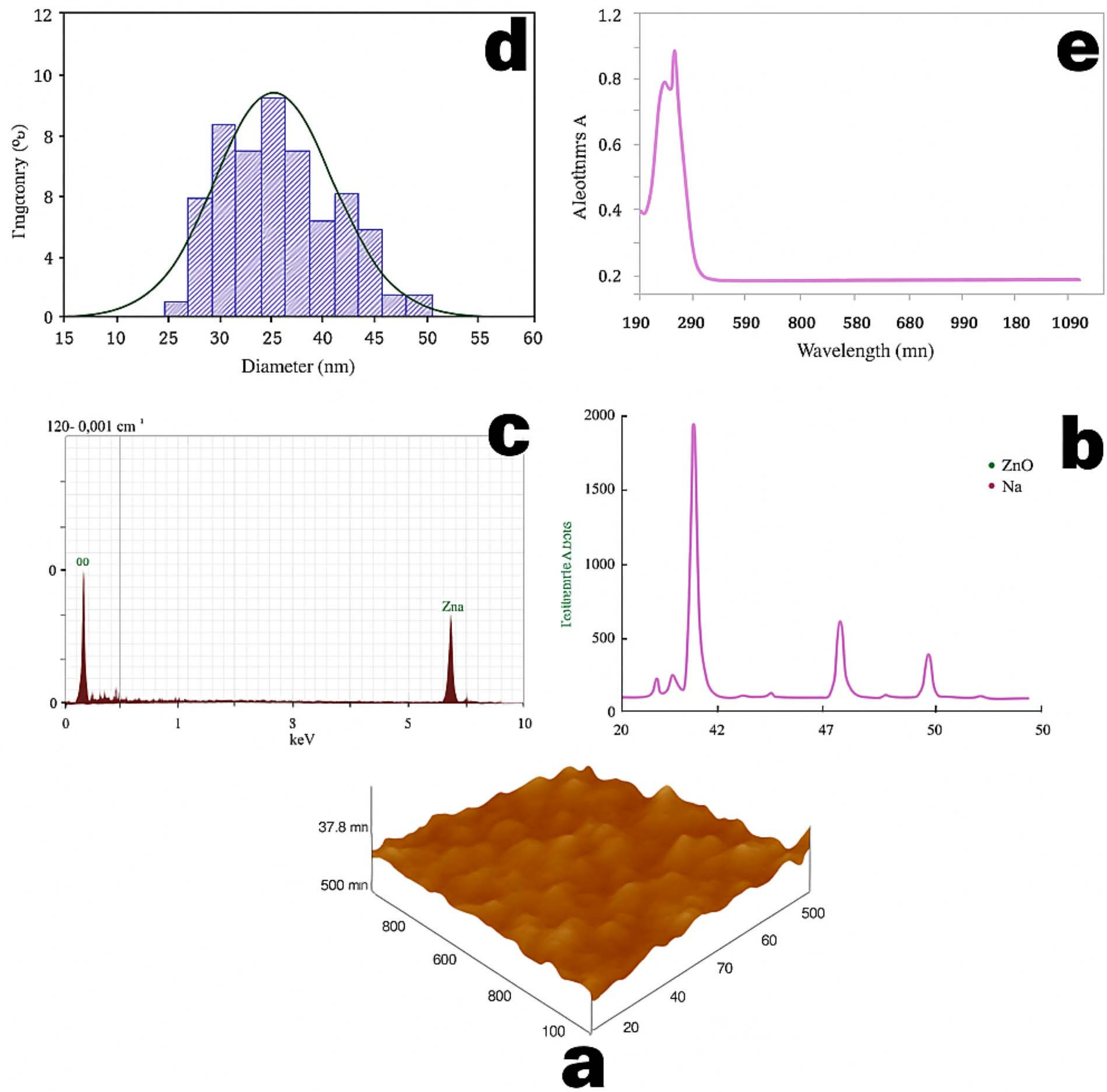

Fig. 2 Characterization of synthesized ZnO nanoparticles (ZnONPs). (a) AFM 3D image of the ZnONPs. (b) XRD spectrum of the ZnONPs, (c) EDAX of the ZnONPs. (d) FESEM of the ZnONPs (e) UV spectrum of the ZnONPs.

against a multidrug-resistant strain of *A. baumannii* isolated from wound infection samples, as shown in (Table 2). The tested concentrations were 1000, 500, 250, 125, and 62.5 μg mL^{-1}. A concentration of 1000 μg mL^{-1} effectively inhibited the growth of the standard control strain, while the inhibitory concentrations for the tested isolates were calculated accordingly. Notably, the multidrug-resistant isolate was inhibited at a concentration of 125 μg mL^{-1}, which is lower than the MIC observed for the control strain.

Table 2 MIC μg ml^{-1} test results ZnONPs, Lfx and Lfx-ZnONPs

Isolate no.	ZnONPs	Lfx	Lfx-ZnONPs
1000 μg mL^{-1}	0.60 ± 0.03	0.54 ± 0.02	0.12 ± 0.01
500 μg mL^{-1}	0.45 ± 0.02	0.40 ± 0.01	0.11 ± 0.01
250 μg mL^{-1}	0.46 ± 0.02	0.31 ± 0.01	0.11 ± 0.01
125 μg mL^{-1}	0.44 ± 0.02	0.27 ± 0.01	0.10 ± 0.01
62.5 μg mL^{-1}	0.36 ± 0.02	0.25 ± 0.01	0.12 ± 0.01

Antifungal activity

The antifungal activity of the synthesized ZnO nanoparticles (ZnONPs) and levofloxacin-loaded ZnONPs (Lfx-ZnONPs) was evaluated using the agar diffusion assay against three *Candida* species: *C. albicans*, *C. glabrata*, and *C. krusei*. Zones of

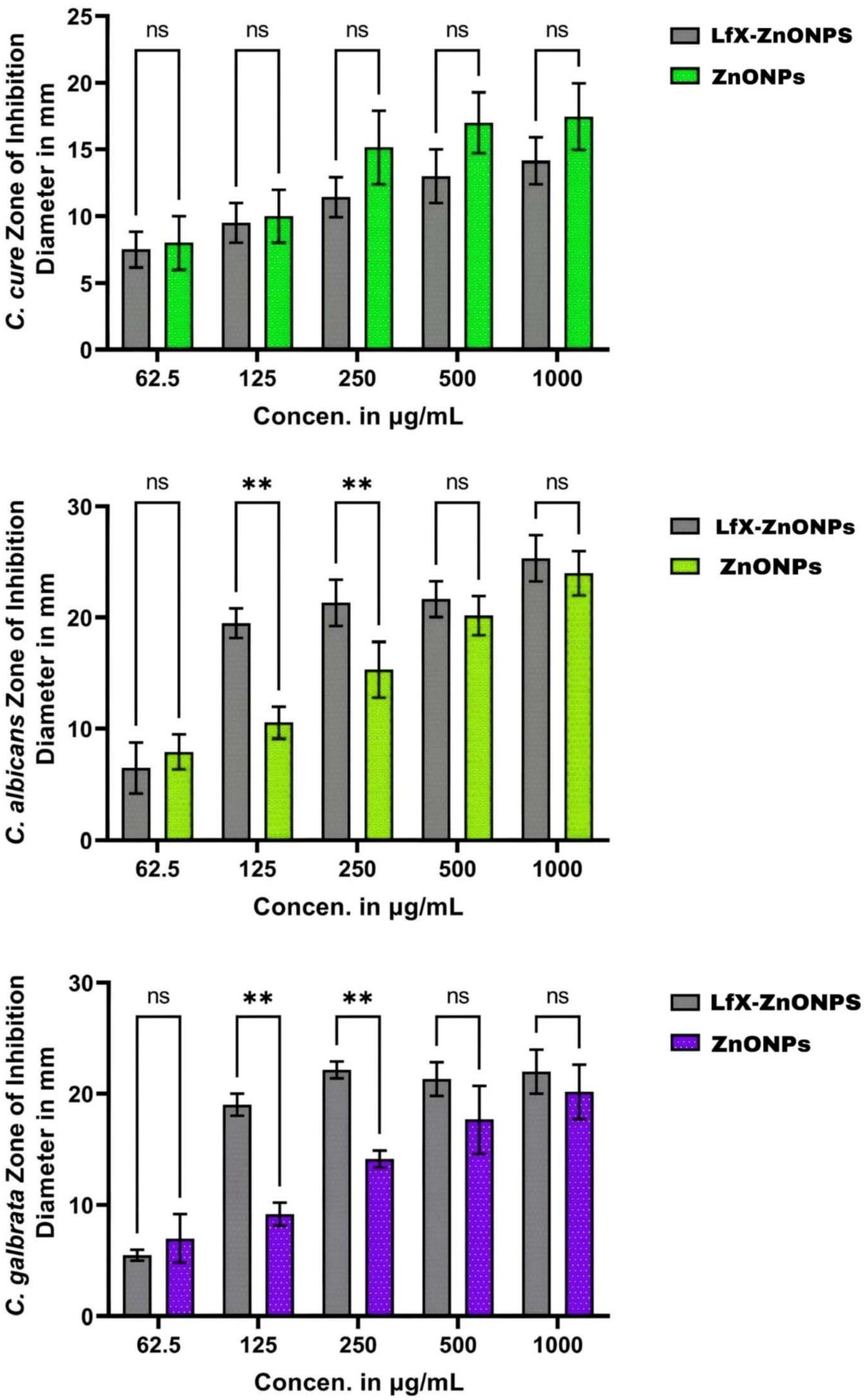

Fig. 3 Inhibition zones of ZnO-NPs against tested *Candida* spp.

inhibition (ZOI) formed around the wells were measured in millimeters (mm) using a zone reader. Both ZnONPs and Lfx-ZnONPs exhibited inhibitory effects against all tested *Candida* species, with the extent of inhibition increasing in a dose-dependent manner as the nanoparticle concentration increased, as illustrated in (Fig. 3). The highest antifungal activity was observed at a ZnONP concentration of 1000 µg mL^{-1}, where *C. albicans* exhibited a ZOI of 22.2 ± 0.2 mm. *C. glabrata* showed a ZOI of 7.6 ± 0.2 mm at the lowest concentration tested (62.5 µg mL^{-1}) and 19.3 ± 0.2 mm at the highest concentration (1000 µg mL^{-1}), while *C. krusei* displayed the lowest response at 62.5 µg mL^{-1} (8.3 ± 0.2 mm). At the maximum dose, Lfx-ZnONPs demonstrated greater antifungal activity than either the pure drug or ZnONPs alone, with ZOIs of 19.5 ± 0.2 mm against *C. albicans* and 12.3 ± 0.2 mm against *C. krusei*. In contrast, *C. glabrata* showed the least response to Lfx-ZnONPs at 62.5 µg mL^{-1} (6.4 ± 0.2 mm), while at intermediate concentrations, *C. albicans* and *C. glabrata* exhibited ZOIs of

Table 3 The percentage of biofilm formation inhibition of isolates in the presence of the ZnONPs, Lfx and Lfx-ZnONPs against *A. baumannii*

Concentration ($\mu g\ mL^{-1}$)	ZnONPs	Lfx	Lfx-ZnONPs	Sig.	*p* Value
1000	13.0 ± 1.0a	12.0 ± 1.0a	11.3 ± 0.6a	NS	0.1447
500	16.0 ± 1.0b	13.7 ± 0.6 ab	12.7 ± 1.5a	*	0.0256
250	19.0 ± 1.0c	15.0 ± 1.0bc	15.0 ± 0.6b	**	0.0025
125	23.0 ± 1.0d	16.3 ± 0.6 cd	16.7 ± 0.6b	**	<0.0001
62.5	28.0 ± 1.0e	18.3 ± 0.6d	20.0 ± 1.0c	**	<0.0001

18.7 ± 0.2 mm and 17.3 ± 0.2 mm, respectively. These results confirm the dose-dependent antifungal efficacy of both ZnONPs and Lfx-ZnONPs against clinically relevant *Candida* species.

Antibiofilm properties of ZnONPs, Lfx and Lfx-ZnONPs

Both ZnONPs and the Lfx-ZnONPs nanocomposite demonstrated significant inhibition of biofilm formation by the tested *A. baumannii* strain, as presented in (Table 3). Notably, the Lfx-ZnONPs nanocomposite exhibited stronger anti-biofilm activity compared to ZnONPs or Lfx alone at equivalent concentrations, which can be attributed to the synergistic effect and enhanced efficacy provided by the presence of ZnO nanoparticles within the composite.

Gene expression of ZnONPs, Lfx, and Lfx-ZnONPs

Subsequently, we evaluated the expression profiles of genes involved in biofilm formation before and after treatment with ZnONPs, Lfx, and Lfx-ZnONPs using RT-PCR. The results demonstrated a significant reduction in the expression of the targeted genes in treated samples compared to untreated controls. Specifically, treatment with ZnO-NPs resulted in a two- to four-fold decrease in *OmpA* gene expression, as illustrated in (Fig. 4).

Histopathology results

Nanoparticles with varying physicochemical properties exhibit distinct toxicological effects, as evidenced by histopathological changes observed in the liver and spleen. In group 1, liver sections were characterized by aggregation of neutrophils within dilated, congested sinusoids and necrosis of hepatocytes (Fig. 5a), while spleen tissue displayed neutrophil infiltration in the congested red pulp accompanied by depletion of white pulp (Fig. 5b). In group 2, liver samples exhibited mild changes, including proliferation of Kupffer cells (Fig. 5c) and mild neutrophil infiltration in the sinusoids, whereas the spleen showed mild hyperplasia of the white pulp (Fig. 5d).

Discussion

Nanoparticles have emerged as a revolutionary platform in antimicrobial therapy, offering solutions to the persistent challenges posed by bacterial and fungal infections.[48] Their unique physicochemical properties-including high surface area to volume ratio, tunable size, and surface charge-enable enhanced interaction with microbial cells, thereby improving the efficacy of conventional antibiotics and antifungal agents. This enhanced interaction facilitates better penetration of biofilms, which are complex microbial communities that exhibit high resistance to standard treatments, thus addressing a critical barrier in infectious disease management.[49]

Recent advances have demonstrated that metal-based nanoparticles, polymeric micelles, and liposomal nanoparticles possess superior biofilm penetration capabilities compared to traditional antibiotics. This is largely due to their ability to disrupt the extracellular polymeric substance matrix of biofilms and deliver antimicrobial agents directly to microbial

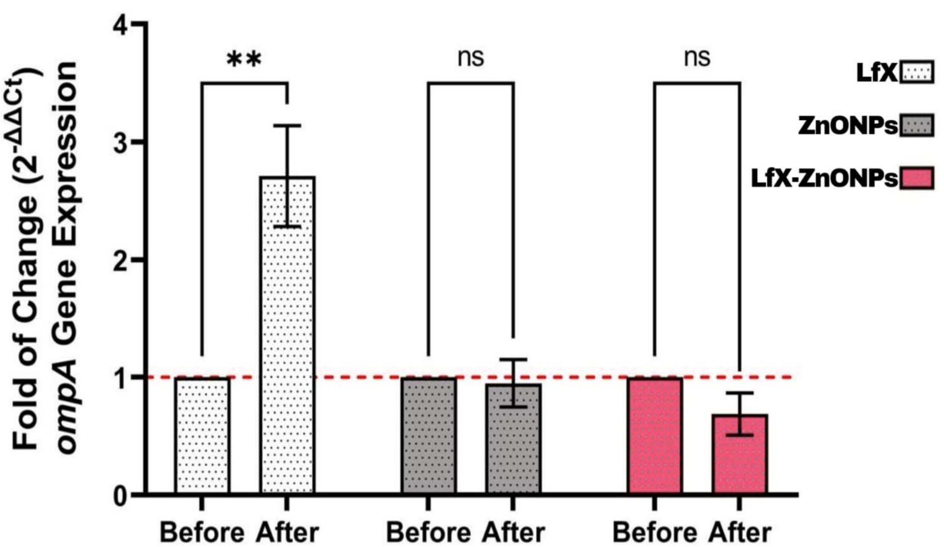

Fig. 4 Fold of change of *OmpA* gene expression in *A. baumannii* before and after treatment with ZnONPs, Lfx, and Lfx-ZnONPs compared with untreated cells. Standard deviation, ($n = 3$).

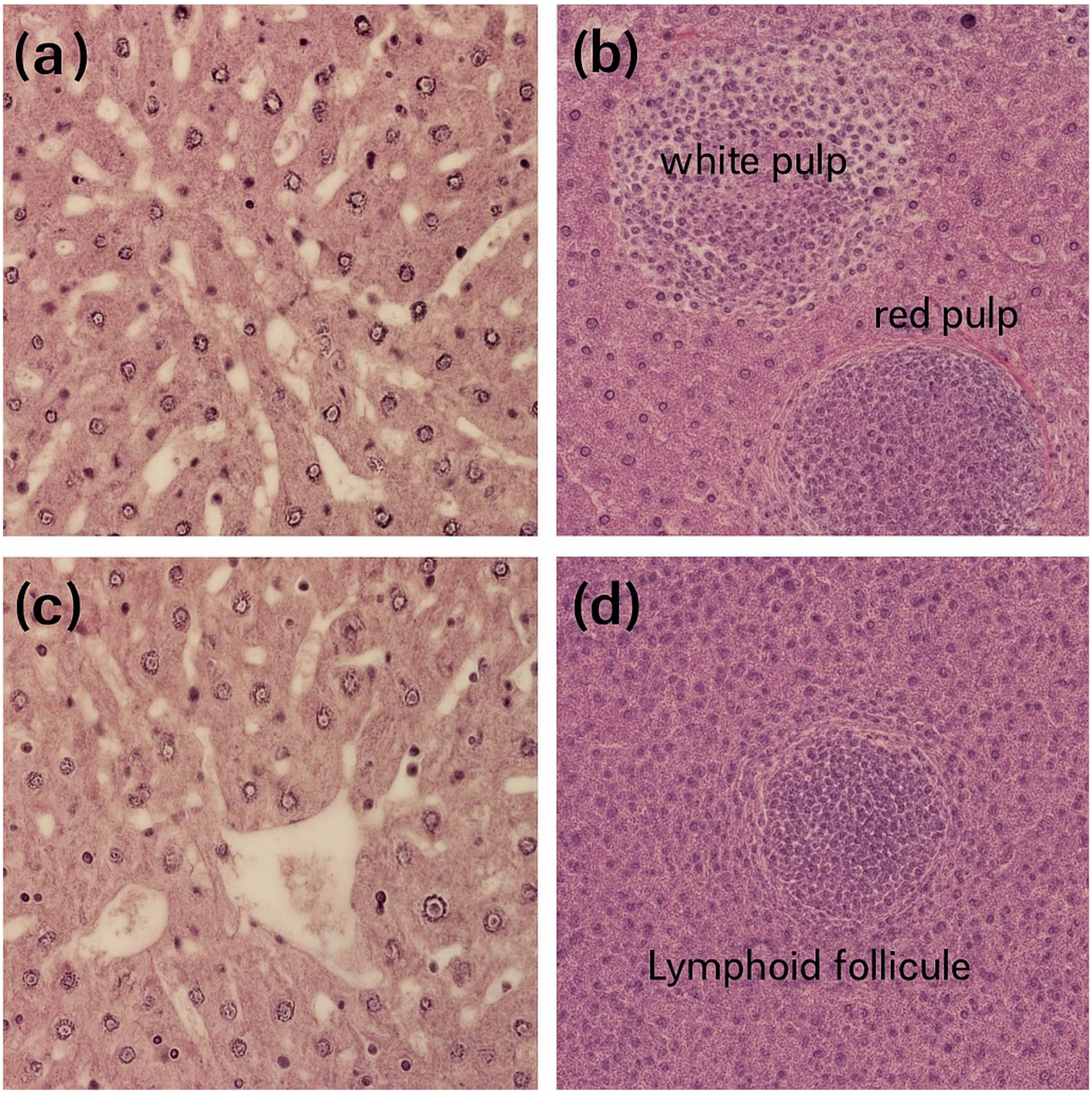

Fig. 5 Histopathological sections of liver and spleen from animals administered 128 μg mL^{-1} of ZnONPs or Lfx-ZnONPs *via* drinking water (H&E stain; 400×). (a) Liver of ZnONP-treated animal showing proliferation of Kupffer cells (arrow). (b) Liver of Lfx-ZnONPs-treated animal showing neutrophil aggregation in dilated, congested sinusoids (yellow arrow) and hepatocyte necrosis (black arrow). (c) Spleen of ZnONP-treated animal exhibiting neutrophil infiltration in congested red pulp and depletion of white pulp. (d) Spleen of Lfx-ZnONPs-treated animal displaying moderate lymphocyte proliferation in the periarteriolar sheath (arrow).

cells. The multi-mechanistic action of nanoparticles which includes physical disruption of cell membranes, generation of reactive oxygen species (ROS), and metal ion release-makes it significantly more difficult for bacteria to develop resistance. This is a crucial advantage in the era of increasing antibiotic resistance, where conventional drugs are becoming less effective.

Moreover, nanoparticles enable targeted drug delivery, which not only enhances therapeutic efficacy but also reduces systemic toxicity. By allowing for lower dosages of antibiotics without compromising effectiveness, nanoparticles minimize adverse side effects and reduce the selective pressure that drives the emergence of resistant strains. This targeted approach is particularly beneficial in treating infections caused by multidrug-resistant organisms, which are a growing global health concern.[50]

In addition to their antimicrobial properties, nanoparticles can be engineered to possess antifungal activity, expanding their therapeutic potential. The current study highlights the successful biosynthesis of zinc oxide nanoparticles (ZnONPs) using environmentally friendly methods involving soybean seed extract, which serves as a reducing and capping agent. This green synthesis approach not only reduces environmental impact but also enhances the biocompatibility of the nanoparticles, making them more suitable for biomedical applications.

(Lfx), a widely used fluoroquinolone antibiotic, was effectively loaded onto ZnONPs to create a nanocomposite with enhanced antibacterial and antifungal properties. The combination leverages the broad-spectrum activity of levofloxacin and the unique mechanisms of ZnONPs, resulting in synergistic effects that improve microbial killing and biofilm inhibition. This is particularly important given the increasing resistance to levofloxacin observed in pathogens such as *Klebsiella pneumoniae*, *Escherichia coli*, *S. aureus*, and *P. aeruginosa*.

The study's findings demonstrate that Lfx-ZnONPs exhibit superior bactericidal and anti-biofilm activities against both Gram-negative and Gram-positive bacteria compared to levofloxacin alone. This enhanced efficacy is attributed to the improved drug delivery and sustained release provided by the nanoparticle carrier, as well as the intrinsic antimicrobial properties of ZnONPs. These results are consistent with previous reports on other metal oxide nanoparticles, such as copper oxide (CuO) nanoparticles loaded with levofloxacin, which have shown increased antibacterial activity and efficacy over standard antibiotics.[51]

Despite the promising therapeutic potential of ZnONPs, concerns regarding their toxicity remain. The current study and previous literature indicate that ZnONPs can induce hepatotoxicity and nephrotoxicity, as evidenced by elevated liver and kidney function markers and histopathological changes in animal models. These toxic effects are dose-dependent and influenced by nanoparticle size and concentration, underscoring the importance of careful dose optimization and thorough toxicological evaluation in the development of nanoparticle-based therapeutics.

Importantly, the concentrations of ZnONPs used in the antifungal assays were within a safe range, with a minimum inhibitory concentration (MIC) of 125 $\mu g\ mL^{-1}$. The Lfx-ZnONPs nanocomposite demonstrated effective antibacterial and antifungal activity at low doses, suggesting a favorable therapeutic index. The synergistic action of zinc oxide ions and levofloxacin not only enhances antimicrobial efficacy but also potentially reduces the required dosage, thereby mitigating toxicity risks.[52]

This study is the first to report the use of levofloxacin loaded ZnONPs as a drug delivery vehicle with potential antifungal applications against pathogenic *Candida* species. The results reveal significant inhibitory effects of both ZnONPs and Lfx-ZnONPs on human pathogenic fungi, highlighting the potential of nanoparticle-based formulations to improve drug availability, enhance efficacy against fungal pathogens, and reduce the likelihood of resistance development.

Furthermore, the environmental and economic benefits of green synthesis methods for nanoparticle production cannot be overstated. Utilizing plant extracts, such as soybean seed extract, as reducing and capping agents offers a sustainable alternative to conventional chemical synthesis, which often involves toxic reagents and harsh conditions. This eco-friendly approach not only reduces the environmental footprint but also enhances the biocompatibility and safety profile of the nanoparticles, making them more suitable for biomedical applications.[53]

The physicochemical characterization of nanoparticles, including size, shape, surface charge, and crystallinity, plays a crucial role in determining their biological activity and toxicity. Techniques such as atomic force microscopy (AFM), field emission scanning electron microscopy (FESEM), energy-dispersive X-ray analysis (EDAX), and X-ray diffraction (XRD) provide detailed insights into these properties, enabling the optimization of nanoparticle synthesis for desired therapeutic outcomes.

In the context of antimicrobial therapy, the size of nanoparticles is particularly important, as smaller particles tend to exhibit higher surface reactivity and better cellular uptake, leading to enhanced antimicrobial effects. However, smaller size may also increase toxicity, necessitating a careful balance between efficacy and safety.[54]

The observed synergistic effects of Lfx-ZnONPs nanocomposites highlight the potential of combining antibiotics with nanoparticles to overcome bacterial resistance mechanisms. By facilitating improved drug delivery and sustained release, nanoparticles can restore the effectiveness of antibiotics that have become less potent due to resistance. This strategy also opens the door to repurposing existing antibiotics, extending their clinical utility.[55]

Moreover, the antifungal activity of ZnONPs and Lfx-ZnONPs against clinically relevant *Candida* species addresses a significant gap in current antifungal therapies. Fungal infections, particularly those caused by *Candida* spp., pose serious health risks, especially in immunocompromised patients. The development of nanoparticle-based antifungal agents offers a promising avenue to enhance treatment efficacy and reduce the emergence of resistant fungal strains.

Toxicological assessments remain a critical component of nanoparticle research. The dose-dependent hepatotoxicity and nephrotoxicity observed in animal models underscore the need for rigorous safety evaluations. Future studies should focus on elucidating the mechanisms underlying nanoparticle-induced toxicity and developing strategies to mitigate adverse effects, such as surface modification or targeted delivery systems.[56]

In addition, the potential immunomodulatory effects of nanoparticles warrant further investigation. Nanoparticles may interact with the immune system in complex ways, potentially enhancing host defense mechanisms or, conversely, triggering undesirable inflammatory responses. Understanding these interactions is essential for the safe and effective clinical translation of nanoparticle-based therapies.[57]

The integration of nanoparticles into clinical practice also requires consideration of regulatory and manufacturing challenges. Standardization of synthesis protocols, quality control measures, and scalability are vital to ensure consistent product quality and safety. Collaborative efforts among researchers, clinicians, and regulatory agencies will be key to overcoming these hurdles.[58]

Beyond antimicrobial applications, the multifunctional nature of nanoparticles opens avenues for their use in diagnostics, imaging, and targeted therapy. The ability to functionalize nanoparticle surfaces with ligands, antibodies, or other targeting moieties allows for precise delivery to specific tissues or cells, minimizing off-target effects and improving treatment outcomes.

To further enhance the clinical potential of levofloxacin-loaded ZnO nanoparticles, future research should focus on developing targeted delivery systems. Functional modifications, such as conjugating targeting ligands (*e.g.*, antibodies, peptides, or small molecules) to the nanoparticle surface, can facilitate selective binding to bacterial cells or infected tissues, thereby increasing therapeutic efficacy and minimizing off target effects. Additionally, encapsulating the nanoparticles within biocompatible polymers or liposomes may improve their stability, circulation time, and controlled release properties. These strategies could enable site-specific drug delivery, reduce systemic toxicity, and help overcome biological barriers such as biofilms. Comprehensive *in vivo* studies are warranted to evaluate the targeting efficiency, pharmacokinetics, and safety of these advanced nano formulations. Ultimately, integrating targeted delivery approaches with biosynthesized Lfx-ZnONPs may accelerate their translation into clinical applications for combating multidrug-resistant infections.

Conclusion

Antibiotic resistance represents a significant global health challenge, threatening the effectiveness of essential medical interventions and undermining the foundation of modern medicine. In this study, we demonstrated that levofloxacin loaded zinc oxide nanoparticles (Lfx-ZnONPs), synthesized using *S. mitis* biomass, exhibit potent antibacterial and antifungal activity against multidrug resistant *A. baumannii* and clinically relevant *Candida* species. The Lfx-ZnONPs not only inhibited planktonic bacterial growth but also showed enhanced efficacy in disrupting biofilm formation and reducing the expression of biofilm associated genes compared to levofloxacin or ZnO nanoparticles alone. While these findings highlight the promise of biosynthesized Lfx-ZnONPs as an alternative to conventional antibiotics, the current work is limited by its *in vitro* and preliminary *in vivo* toxicity assessments, a restricted range of tested pathogens, and the need for further mechanistic and pharmacokinetic studies. Future research should focus on optimizing nanoparticle formulations for targeted delivery, minimizing toxicity, expanding the spectrum of tested pathogens, and conducting comprehensive *in vivo* studies to validate clinical potential. Overall, our results provide a foundation for the development of nanoparticle based antimicrobial therapies and support further exploration of Lfx-ZnONPs as a novel approach to address the growing challenge of antibiotic resistance.

Ethical statement

This research was approved by the Committee of Ethical Standards in the College of Sciences/University of Baghdad. The study protocol, subject information, and permission form were reviewed and approved by a local ethics committee the document number April 9, 2024 Ref: CSEC/0425/0083.

Conflicts of interest

The authors declare no competing interests.

Data availability

All data supporting the findings of this study are available within the article and its SI file. See DOI: **https://doi.org/10.1039/d5ra03081a**.

References

1 M. Ferri, *et al.*, Antimicrobial resistance: A global emerging threat to public health systems, *Crit. Rev. Food Sci. Nutr.*, 2017, **57**(13), 2857–2876.
2 T. M. Coque, *et al.*, Antimicrobial resistance in the global health network: known unknowns and challenges for efficient responses in the 21st century, *Microorganisms*, 2023, **11**(4), 1050.
3 P. Dadgostar, Antimicrobial resistance: implications and costs, *Infect. Drug Resist.*, 2019, 3903–3910.
4 M. N. Temgoua, *et al.*, Coronavirus disease 2019 (COVID-19) as a multi-systemic disease and its impact in low-and middle-income countries (LMICs), *SN Compr. Clin. Med.*, 2020, **2**, 1377–1387.
5 B. Holman, Methods, and Decisions, Humbug, the Council of Pharmacy and Chemistry, and the Origin of "The Blind Test" of Therapeutic Efficacy, *Uncertainty in Pharmacology*, 2020, pp. 397–416.
6 S. J. Dunachie, N. P. Day and C. Dolecek, The challenges of estimating the human global burden of disease of antimicrobial resistant bacteria, *Curr. Opin. Microbiol.*, 2020, **57**, 95–101.
7 M. D. Pezzani, *et al.*, Methodological quality of studies evaluating the burden of drug-resistant infections in humans due to the WHO Global Antimicrobial Resistance Surveillance System target bacteria, *Clin. Microbiol. Infect.*, 2021, **27**(5), 687–696.
8 Z.-Q. Xu, M. T. Flavin and J. Flavin, Combating multidrug-resistant Gram-negative bacterial infections, *Expet Opin. Invest. Drugs*, 2014, **23**(2), 163–182.
9 S. K. Ali, *et al.*, Assessment of antimicrobial activity and GC-MS using culture filtrate of local marine Bacillus strains, *J. Environ. Sci. Health, Part B*, 2024, **59**(7), 399–416.
10 A. Tarín-Pelló, B. Suay-García and M.-T. Pérez-Gracia, Antibiotic resistant bacteria: current situation and treatment options to accelerate the development of a new antimicrobial arsenal, *Expert Rev. Anti-Infect. Ther.*, 2022, **20**(8), 1095–1108.
11 L. S. Roope, *et al.*, The challenge of antimicrobial resistance: what economics can contribute, *Science*, 2019, **364**(6435), eaau4679.
12 J. Abranches, *et al.*, Biology of oral streptococci, *Microbiol. Spectr.*, 2018, **6**(5), DOI: **10.1128/microbiolspec.gpp3-0042-2018**.
13 J. J. Baty, S. N. Stoner and J. A. Scoffield, Oral commensal streptococci: gatekeepers of the oral cavity, *J. Bacteriol.*, 2022, **204**(11), e00257–22.
14 H. S. Mohamed, *et al.*, Antibacterial and anti-tumor properties of marine posidonoia oceanica leaf extracts, *J. Herbs, Spices, Med. Plants*, 2025, **31**(3), 268–290.

15 E. Mathieu, *et al.*, An isolate of Streptococcus mitis displayed in Vitro Antimicrobial Activity and Deleterious Effect in a preclinical model of lung infection, *Nutrients*, 2023, **15**(2), 263.
16 S. K. Ali, *et al.*, Chemical Analysis and Health Benefits of a Novel Polysaccharide Produced by Paenibacillus mucilaginosus: SK Ali et al, *Curr. Microbiol.*, 2025, **82**(7), 326.
17 J. Borralho, *et al.*, Inhibition of pneumococcal growth and biofilm formation by human isolates of Streptococcus mitis and Streptococcus oralis, *Appl. Environ. Microbiol.*, 2025, **91**(3), e0133624.
18 M. Kilian and H. Tettelin, Identification of virulence-associated properties by comparative genome analysis of Streptococcus pneumoniae, S. pseudopneumoniae, S. mitis, three S. oralis subspecies, and S. infantis, *mBio*, 2019, **10**(5), e0198519, DOI: 10.1128/mbio.01985-19.
19 A. P. Ramos, *et al.*, Biomedical applications of nanotechnology, *Biophys. Rev.*, 2017, **9**(2), 79–89.
20 Y. Khan, *et al.*, Classification, synthetic, and characterization approaches to nanoparticles, and their applications in various fields of nanotechnology: a review, *Catalysts*, 2022, **12**(11), 1386.
21 H. S. Mohamed, *et al.*, Nano metal oxide impregnated Chitosan-4-nitroacetophenone for industrial dye removal, *Int. J. Environ. Anal. Chem.*, 2021, **101**(13), 1850–1877.
22 F. Mohamed, *et al.*, Adsorptive potential of dispersible chitosan-coated biogenic iron oxide nanocomposite for enhanced anti-bacterial activity against gram-positive and gram-negative bacterial pathogens, *Anal. Chem. Lett.*, 2024, **14**(5), 693–707.
23 C. Fang and M. Zhang, Nanoparticle-based theragnostics: Integrating diagnostic and therapeutic potentials in nanomedicine, *J. Controlled Release*, 2010, **146**(1), 2.
24 O. T. Nemr, *et al.*, Investigating the anticancer and antioxidant potentials of a polymer-grafted sodium alginate composite embedded with CuO and TiO2 Nanoparticles, *J. Polym. Environ.*, 2024, **32**(6), 2713–2728.
25 A. Yusuf, *et al.*, Nanoparticles as drug delivery systems: a review of the implication of nanoparticles' physicochemical properties on responses in biological systems, *Polymers*, 2023, **15**(7), 1596.
26 E. M. Azzam, *et al.*, Removal of iron (II) from wastewater in oil field using 3-(p-methyl) phenyl-5-thionyl-1, 2, 4-triazoline assembled on silver nanoparticles, *Desalin. Water Treat.*, 2019, **142**, 244–251.
27 S. Parveen, R. Misra and S. K. Sahoo, Nanoparticles: a boon to drug delivery, therapeutics, diagnostics and imaging, *Nanomedicine*, 2017, 47–98.
28 M. E. Caldorera-Moore, W. B. Liechty and N. A. Peppas, Responsive theranostic systems: integration of diagnostic imaging agents and responsive controlled release drug delivery carriers, *Acc. Chem. Res.*, 2011, **44**(10), 1061–1070.
29 A. S. Angel, Green Synthesis Methods for Metallic Zinc Oxide Nanoparticles: A Sustainable Angle, *Synthesizing and Characterizing Plant-Mediated Biocompatible Metal Nanoparticles*, 2025, p. 63.
30 A. Jain and K. Bhise, Green Synthesis Methods for Metallic Zinc Oxide Nanoparticles: A Sustainable Angle, in *Synthesizing and Characterizing Plant-Mediated Biocompatible Metal Nanoparticles*, IGI Global, 2025, pp. 63–90.
31 M. Ijaz, *et al.*, A review on antibacterial properties of biologically synthesized zinc oxide nanostructures, *J. Inorg. Organomet. Polym. Mater.*, 2020, **30**, 2815–2826.
32 A. Punnoose, *et al.*, Cytotoxicity of ZnO nanoparticles can be tailored by modifying their surface structure: a green chemistry approach for safer nanomaterials, *ACS Sustainable Chem. Eng.*, 2014, **2**(7), 1666–1673.
33 A. Tereshchenko, *et al.*, Optical biosensors based on ZnO nanostructures: advantages and perspectives. A review, *Sens. Actuators, B*, 2016, **229**, 664–677.
34 F. M. AlKandari, *et al.*, Protective effects of propolis and chitosan nanoparticles against ibuprofen-induced hepatotoxicity in albino rats, *Diseases*, 2024, **12**(3), 49.
35 I. Kim, *et al.*, ZnO nanostructures in active antibacterial food packaging: Preparation methods, antimicrobial mechanisms, safety issues, future prospects, and challenges, *Food Rev. Int.*, 2022, **38**(4), 537–565.
36 S. Shaikh, *et al.*, Mechanistic insights into the antimicrobial actions of metallic nanoparticles and their implications for multidrug resistance, *Int. J. Mol. Sci.*, 2019, **20**(10), 2468.
37 T. Abdullah, *et al.*, Recent Advances in the Development of Metal/Metal Oxide Nanoparticle and Antibiotic Conjugates (MNP–Antibiotics) to Address Antibiotic Resistance: Review and Perspective, *Int. J. Mol. Sci.*, 2024, **25**(16), 8915.
38 S. Weinberg, *et al.*, Control and management of multidrug resistant Acinetobacter baumannii: a review of the evidence and proposal of novel approaches, *Infection Prevention in Practice*, 2020, **2**(3), 100077.
39 K. Khorsandi, *et al.*, A mechanistic perspective on targeting bacterial drug resistance with nanoparticles, *J. Drug Targeting*, 2021, **29**(9), 941–959.
40 N. H. Faiq and M. E. Ahmed, Effect of biosynthesized zinc oxide nanoparticles on phenotypic and genotypic biofilm formation of Proteus mirabilis, *Baghdad Sci. J.*, 2024, **21**(3), 0894.
41 S. H. Seddiq, A. M. Zyara and M. E. Ahmed, Evaluation the antimicrobial action of kiwifruit zinc oxide nanoparticles against Staphylococcus aureus isolated from cosmetics tools, *BioNanoScience*, 2023, **13**(3), 1140–1149.
42 E. O. Köse, In vitro activity of carvacrol in combination with meropenem against carbapenem-resistant Klebsiella pneumoniae, *Folia Microbiol.*, 2022, **67**(1), 143–156.
43 F. Thakral, *et al.*, Synergistic anti-bacterial effects of green synthesized zinc oxide nanoparticles with levofloxacin, *J. King Saud Univ., Sci.*, 2023, **35**(8), 102905.
44 Z. A. H. Al-Rubaie, *et al.*, Evaluation of the antibiofilm, effects the related mechanisms on colistin-resistant Pseudomonas aeruginosa: antibiofilm and colistin-resistant Pseudomonas aeruginosa, *J. Med. Health Sci.*, 2025, **2**(1), 55–70.
45 M. Basumatari, *et al.*, Musa balbisiana Colla pseudostem biowaste mediated zinc oxide nanoparticles: their

antibiofilm and antibacterial potentiality, *Curr. Res. Green Sustainable Chem.*, 2021, **4**, 100048.

46 J. S. Yuan, A. Reed, F. Chen and C. N. Stewart Jr, Statistical analysis of real-time PCR data, *BMC Bioinf.*, 2006, **7**(1), 85.

47 S. Mahmood, The prevalence of (ompa, csue) genes among biofilm producer acinetobacter baumannii isolates, *Iraqi J. Agric. Sci.*, 2024, **55**(5), 1720–1727.

48 G. Muteeb, *et al.*, Origin of antibiotics and antibiotic resistance, and their impacts on drug development: a narrative review, *Pharmaceuticals*, 2023, **16**(11), 1615.

49 S. Bharti and A. Kumar, Nanotechnology in Targeted Delivery of Antimicrobials and Overcoming Resistance, *BioNanoScience*, 2025, **15**(1), 1–22.

50 B. F. Finina and A. K. Mersha, Nano-enabled antimicrobial thin films: design and mechanism of action, *RSC Adv.*, 2024, **14**(8), 5290–5308.

51 M. Naseer, *et al.*, Green route to synthesize zinc oxide nanoparticles using leaf extracts of Cassia fistula and Melia azadarach and their antibacterial potential, *Sci. Rep.*, 2020, **10**(1), 9055.

52 Z. Saleem, *et al.*, Point prevalence surveys of health-care-associated infections: a systematic review, *Pathog. Global Health*, 2019, **113**(4), 191–205.

53 N. H. Faiq and M. E. Ahmed, Inhibitory effects of biosynthesized copper nanoparticles on biofilm formation of Proteus mirabilis, *Iraqi J. Sci.*, 2024, 65–78.

54 E. E. Imade, *et al.*, Green synthesis of zinc oxide nanoparticles using plantain peel extracts and the evaluation of their antibacterial activity, *Sci. Afr.*, 2022, **16**, e01152.

55 A. Jabeen, *et al.*, Biogenic synthesis of levofloxacin-loaded copper oxide nanoparticles using Cymbopogon citratus: a green approach for effective antibacterial applications, *Heliyon*, 2024, **10**(6).

56 M. H. Hassan, *et al.*, Toxicological screening of zinc oxide nanoparticles in mongrel dogs after seven days of repeated subcutaneous injections, *BMC Vet. Res.*, 2024, **20**(1), 476.

57 B. E. Aboulhoda, *et al.*, Hepatotoxic effect of oral zinc oxide nanoparticles and the ameliorating role of selenium in rats: a histological, immunohistochemical and molecular study, *Tissue Cell*, 2020, **67**, 101441.

58 O. A. Ghareeb, Toxicopathological effects of zinc oxide nanoparticles on the liver function and preventive role of silymarin in vivo, *Indian J. Forensic Med. Toxicol.*, 2021, **15**(2), 3212–3217.